



Doc Number: MI-0245
Version: 1.1

Some Additional Information for Dipole and Quadrupole Power Supply Control

Bruce C. Brown
Beams Division, Main Injector Department
*Fermi National Accelerator Laboratory **
P.O. Box 500
Batavia, Illinois 60510

9/4/98

Contents

1	Introduction	2
2	Quadrupole Strength and Tune Control Model	2
3	Applying Corrections for Tune Control	4
3.1	Main Ring Traditions	5
3.2	Considerations for Tune Control Software Design	6
4	Observations on Saturation and Hysteresis	6
5	Hysteresis Fitting	11
5.1	General Properties	11
5.2	Measured Hysteresis Response and Fits	12
5.3	Discussion of Fit Results	17
6	Conclusions	18

*Operated by the Universities Research Association under contract with the U. S. Department of Energy

Abstract

The efforts to describe the dipole and quadrupole magnet performance for Main Injector operation continue. In this note we will examine the relations between tune and magnet strengths, use measured data to give explicit, if crude numbers for magnet operation with various ramp conditions and examine the some crude fits to hysteresis measurements.

1 Introduction

The requirements for focusing and chromaticity control in the Main Injector were reviewed in Fermilab-Conf-97/147[1] with additional details developed in MI-0211[2]. Work continues to provide explicit guidance for Main Injector power supply control programming. This note will provide an update on ongoing efforts.

2 Quadrupole Strength and Tune Control Model

To provide the correct gradient strengths for Main Injector operation, we examine the relation between gradient strength on focusing and defocusing buses *vs.* the tune achieved in Lattice MI19. In general terms, we know that the the horizontal and vertical tunes are related to the quadrupole strength of two families of quadrupoles. If we express this focusing strength in geometric terms (momentum independent) and use a linear expansion of this relation about the operating point, we should describe it with a linear matrix equation. Let us determine this function using the MI19 lattice model¹.

Dave Johnson has used the MAD lattice modeling code and established the relations between tune and focusing (k_f, k_d) for an array of tunes (ν_x, ν_y) near the operating point. The design lattice used is identified as MI19. These results were described in MI-0185[3]. He provided a description of these results there, but we choose instead to re-examine the calculated results and provide a description which we believe to be more generally useful. The tune results which Dave obtained² are reported in Table 1. We fit them to

¹Some of the following material has been circulated privately as BCB-98-001, 6/9/98.

²Private communication from David E. Johnson, MI#3 Logbook, p.118.

ν_x	ν_y	k_f	k_d
26.425	25.415	0.0406811	-0.039808
26.435	25.415	0.0406913	-0.03981
26.425	25.425	0.0406830	-0.039818
26.435	25.425	0.0406932	-0.03982
26.415	25.415	0.0406709	-0.039806
26.425	25.405	0.0406793	-0.039798

Table 1: Calculated quadrupole strengths k_f (focusing bus), k_d (defocusing bus) of IQB quadrupoles in the MI19 lattice for the specified tune values shown in Columns 1 and 2. k_f and k_d are specified in unit of m^{-2} . These results were obtained by Dave Johnson from MAD simulations.

a bilinear equation,

$$\begin{pmatrix} \nu_x \\ \nu_y \end{pmatrix} = \begin{pmatrix} Q_{11} & Q_{12} \\ Q_{21} & Q_{22} \end{pmatrix} \begin{pmatrix} k_{1f} \\ k_{1d} \end{pmatrix} + \begin{pmatrix} \nu_{0x} \\ \nu_{0y} \end{pmatrix}. \quad (1)$$

Fits to these data³ give the parameters of this equation as follows:

$$\begin{pmatrix} \nu_x \\ \nu_y \end{pmatrix} = \begin{pmatrix} 1014.17 & 186.132 \\ -197.2 & -1028.26 \end{pmatrix} \begin{pmatrix} k_{1f} \\ k_{1d} \end{pmatrix} + \begin{pmatrix} -7.42307 \\ 7.4951 \end{pmatrix}. \quad (2)$$

Since this is a linear expansion about the operating point, the inverse relation is also easily available in the form:

$$\begin{pmatrix} k_{1f} \\ k_{1d} \end{pmatrix} = \begin{pmatrix} K_{11} & K_{12} \\ K_{21} & K_{22} \end{pmatrix} \begin{pmatrix} \nu_x \\ \nu_y \end{pmatrix} + \begin{pmatrix} k_{01f} \\ k_{01d} \end{pmatrix}. \quad (3)$$

Fit results in this form take the values

$$\begin{pmatrix} k_{1f} \\ k_{1d} \end{pmatrix} = \begin{pmatrix} 0.001022 & 0.000185 \\ -0.000196 & -0.001008 \end{pmatrix} \begin{pmatrix} \nu_x \\ \nu_y \end{pmatrix} + \begin{pmatrix} 0.008973 \\ -0.00901 \end{pmatrix}. \quad (4)$$

The two matrices are inverses so their product should be the unit matrix. This has been confirmed. The errors are of order 10^{-6} .

We note that a matrix which is accurate for small tune deviations need only be supplemented by an offset (constants) to fully describe the required

³Stan Pruss used DataDesk to produce these fit results. The fits show 100% correlation which implies that the linear dependence fully accounts for the data over the limit range of variation which was explored.

strength in the useful operating region. We then examine ways to apply corrections based on machine measurements in order to create a coherent plan to use for machine operation.

3 Applying Corrections for Tune Control

The actual machine will only approximately match the design described by $\underline{k}_1 = \underline{K} \underline{\nu} + \underline{k}0_1$ or its inverse. Effects due to component placement as well as the cumulative effect of small magnet measurement errors assure that we will not achieve precisely the beta functions of the design lattice. The response of the tune to the quadrupole focusing will be different than the predictions of the design⁴. The above equations will need to be supplemented by machine measurements to achieve the desired precision of tune control.

The desired working point, (ν_x, ν_y) , will be determined by observed machine operation (probably losses and emittance). It will probably be close to but different from the design tune of (26.425, 25.415). We would like to examine how measured tune values can be most effectively analyzed to provide control parameters for setting the quadrupole currents.

We can, at least in principle, make measurements at fixed momentum of the tune function at a set of tunes near the design operating point. We would operate the machine at various tune values and then determine the actual tune achieved by various (k_f, k_d) values. Suppose we use these measurements to establish the measured tune equation, $\underline{k}_{1m} = \underline{K}_m \underline{\nu}_m + \underline{k}0_{1m}$. How shall we employ these measured results in combination with the design parameters to minimize the sensitivity of this operation to various unknown factors?

Let us consider differences between measured and design parameters. Let $\delta \underline{k}_1 = \underline{k}_{1m} - \underline{k}_{1d}$, $\delta \underline{\nu} = \underline{\nu}_m - \underline{\nu}_d$, and $\delta \underline{k}0_1 = \underline{k}0_{1m} - \underline{k}0_1$. We begin with

$$\underline{k}_{1m} = \underline{K}_m \underline{\nu}_m + \underline{k}0_{1m} \quad (5)$$

$$\underline{k}_{1d} = \underline{K} \underline{\nu}_d + \underline{k}0_{1d} \quad (6)$$

where the d subscript signifies the design point. Taking differences we have

$$\delta \underline{k}_1 = \underline{K}_m \underline{\nu}_m - \underline{K} \underline{\nu}_d + \delta \underline{k}0_1 \quad (7)$$

⁴The MI19 Lattice model which Dave Johnson used employed the design properties of the magnet, without knowledge of the magnet to magnet variation. The strength ratio between 84", 100" and 116" magnets is different at low fields and at high fields (above 120 GeV/c).

$$\delta \underline{k}_1 = \underline{K}_m (\underline{\nu}_m - \underline{\nu}_d) + (\underline{K}_m - \underline{K}) \underline{\nu}_d + \delta \underline{k}0_1 \quad (8)$$

letting $\underline{K}' = \underline{K}_m - \underline{K}$ we have

$$\delta \underline{k}_1 = \underline{K}_m \delta \underline{\nu} + \underline{K}' \underline{\nu}_d + \delta \underline{k}0_1 \quad (9)$$

Alternatively, we can recombine terms to show

$$\delta \underline{k}_1 = \underline{K} \delta \underline{\nu} + \underline{K}' \underline{\nu}_m + \delta \underline{k}0_1 \quad (10)$$

3.1 Main Ring Traditions

The quadrupole control in the Main Ring was based on a sensitivity matrix (same principle as \underline{K}_m or \underline{K}) for relating desired tune changes to the required current changes, and a set of measured tunes and currents which were stored in a table keyed on the dipole current which was called the *calibration* table. Compared with our understanding of Main Injector requirements, this has the disadvantage, in principle, that the relation between fields (and the resulting \underline{k}_1) is dependent on magnet history due to hysteresis. We are committed to attempting to make the hysteretic effect repeatable among different ramps so perhaps we can follow this example. Let us assume that the *calibration* table gives a set of tunes for given dipole and quadrupole currents. We can express this result in the notation used here as

$$\underline{k}_{1m} = \underline{K}_m \underline{\nu}_m + \underline{k}0_{1m} \quad (11)$$

and we assume that if the specified operational tune sought is $\underline{\nu}_s$, we can achieve this tune by changing the focusing by

$$\delta \underline{k}_1 = \underline{K}_m (\underline{\nu}_s - \underline{\nu}_m) \quad (12)$$

In succeeding sections we will examine some hysteresis data. The limitations of the calibration table approach due to hysteretic differences in the relation between field and current will be made explicit there. A principle limitation of the *calibration* table for tune control is that it is defined as a single current-dependent table which applies to all ramps. To add further control, one will need to explicitly subtract the results which this feature generates to permit a time-dependent control function to be implemented.

3.2 Considerations for Tune Control Software Design

In defining the software for Main Injector ramps, the following features have been identified for consideration:

1. It is very important that the tune achieved for a specified ramp be very nearly the tune specified and displayed.
2. One might wish to have easy access also to the
 - (a) the design nominal tune
 - (b) the measured nominal tune
 - (c) the specified tune change

so that the the relation between the model, measurements and specified tune are well understood.

3. The matrix relating tune to focusing can only be measured at at most a few momenta. It is likely that the differences between the design (\underline{K}) and measured (\underline{K}_m) matrices are small such that the design matrix is sufficient for initial implementation.
4. It is desirable to preserve in the control information some clarity as to the degree to which the underlying lattice model is matched by the observed machine properties. Similarly, it is desirable to see what important features change as a function of momentum. For these reasons, we should employ momentum-independent focusing functions where possible (rather than the measured magnetic fields) and should display δk_1 , δk_{0_1} and \underline{K}' as a function of momentum.
5. Although measurements at several tunes settings at a fixed momentum are likely to be available at only a few settings, using equations 9 or 10, we can analyze measurements at a single tune setting, extracting only a value for δk_{0_1} which can be tabulated as a function of momentum and used to achieve a good description of the machine.

Efforts to complete the tune control software are now underway.

4 Observations on Saturation and Hysteresis

Although measurements exist on all MI dipole and quadrupole magnets and hysteresis studies have been performed on one or more magnets of each type,

the analysis of this information is still incomplete. In order to expose some of the issues which will affect power supply regulation and control design, we will examine here some of the current ratios and differences which are important. For simplicity, we choose to interpolate measured data (simple, linear interpolation) rather than use the fitted data shown later in this document. Since we are using only one magnet of each type, we should not expect to match precisely the final results which will represent the whole ring. The magnets are all like to about 0.5% worst case and typically much better. As will be noted, there is some data in which we will use which is not quite right but the general properties which are of interest will still be apparent.

Main Injector Ramp Properties

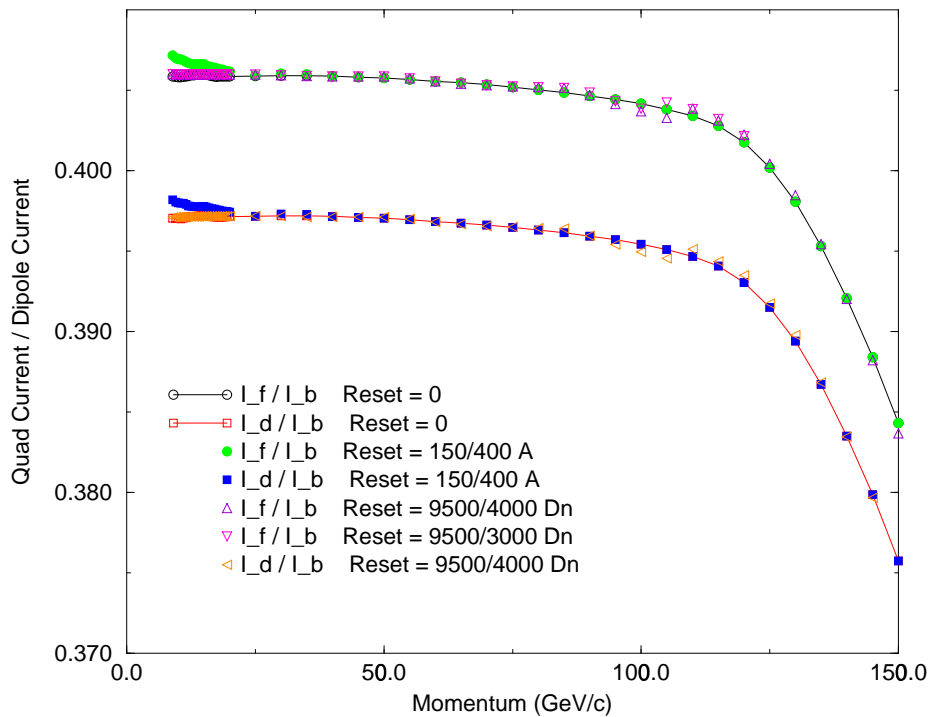


Figure 1: Ratio of Quadrupole to Dipole current for F and D quad buses.

Hysteresis studies of IDA114-0 and IQB310-1 will be used for these illustrations. Ramp tables were constructed in a spreadsheet program using 0.5 GeV/c steps in momentum from injection to 20 GeV/c and 5.0 GeV/c steps from 20 - 150 GeV/c. For each momentum and for the design tune, (26.425, 25.415), the strengths required for IDA and IQB magnets were calculated. The dipole strength was calculated using Equation 3 of MI-0211 while the quadrupole strength used Equation 4 along with Equation 4 of Fermilab-Conf-97/147[1]. $L_{eff} = 2.1176m$ was used for the Quadrupole effective length per MI-0185[3]. The required current for each desired strength was obtained by interpolating between the values measured. Three ramp conditions were considered: Upramp reset at 0 A (dipole and quadrupole), Upramp reset at 400 A for dipoles and 150 A for quadrupoles, and down-ramp reset at the measurement peak current of 9500 A for dipoles and 4000 A for quadrupoles. In addition to these primary values (p, 3 strengths, and 9 currents), a number of ratios and differences were tabulated in the spreadsheet.

To understand the control requirements we consider the relations between the dipole bus current and the two quadrupole bus currents as a function of momentum. In Figure 1 we plot the ratio of quadrupole to dipole current for 3 ramp conditions. These are simply example conditions, not selected as particularly desirable. We see that when viewed as a ratio, the up ramp and down ramp ratios are quite similar (differing by 4×10^{-4} or less over most of the momentum range). However, for the data with higher resets, the ratio changes (differences between the ratios with 0 reset and the higher resets are as large as 30×10^{-4} near injection, approaching no difference at about 20 GeV/c).

This information can be displayed to illustrate another feature of the planned hardware. For control of the quadrupole current, a transductor is provided which compares 2 times the dipole current with 5 times the quadrupole current. In the Main Ring the comparable transductor compared directly the dipole and quadrupole currents, which were comparable at all operating conditions. This provided two benefits: the quadrupole current was regulated to match excursions in the dipole regulation, permitting improved tune control, while the close matching of the two currents permitted one to regulate the quadrupole current from a source whose observed range was small compared to the quadrupole dynamic range. Presumably, the cross-regulation feature will be preserved. However, saturation differences will limit the ability to maintain a very small range for the regulation signal. In Figure 2 we show the transductor signal for the focusing quad bus

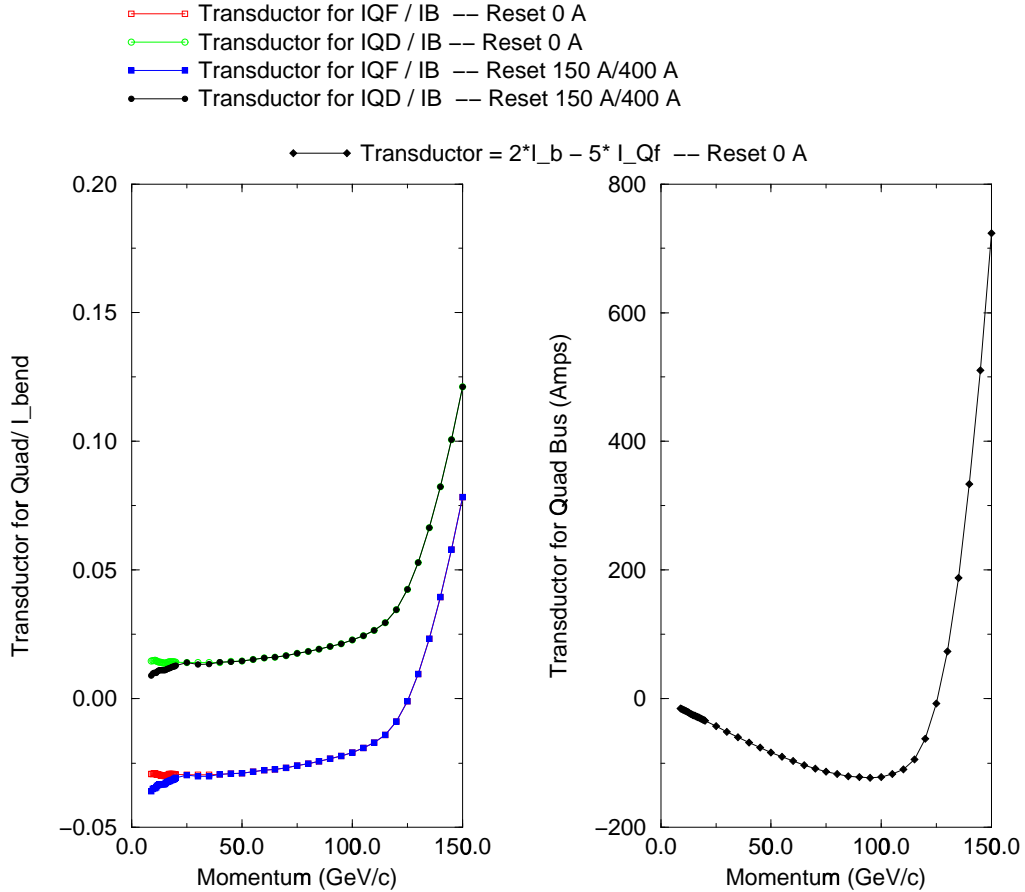


Figure 2: Signal in Amperes expected on 2:5 ratio transductor for Quadrupole Control. Transductor uses outputs of dipole and quadrupole buses with winding ratios of 2 turns for Dipole to 5 turns for F and D quad buses. Left graph has signal in amperes divided by dipole current.

on the right. On the left we show the transductor signal for various ramps for both the focusing and defocusing buses but we divide by the dipole current to reduce the required range of the plot. We see that the match works well at low field. A fifth of the transductor signal should be compared to the quadrupole current. At low field it is one about 1.4% of the quad signal for the focusing bus and 0.7% for the defocusing bus. But as saturation sets in we see that the quads saturate faster than the dipoles. If we only had Main Ring Quads (IQB's) we would find that the high field transductor signal

corresponds to 150 or 230 A at 150 GeV/c which is 4% to 6% of the respective quadrupole current. There is more saturation in the IQC and IQD quadrupoles due to the lower permeability of the Main Injector project steel. This will reduce this saturation difference between dipoles and quadrupole since the long magnets do provide a significant fraction of the focusing in the ring.

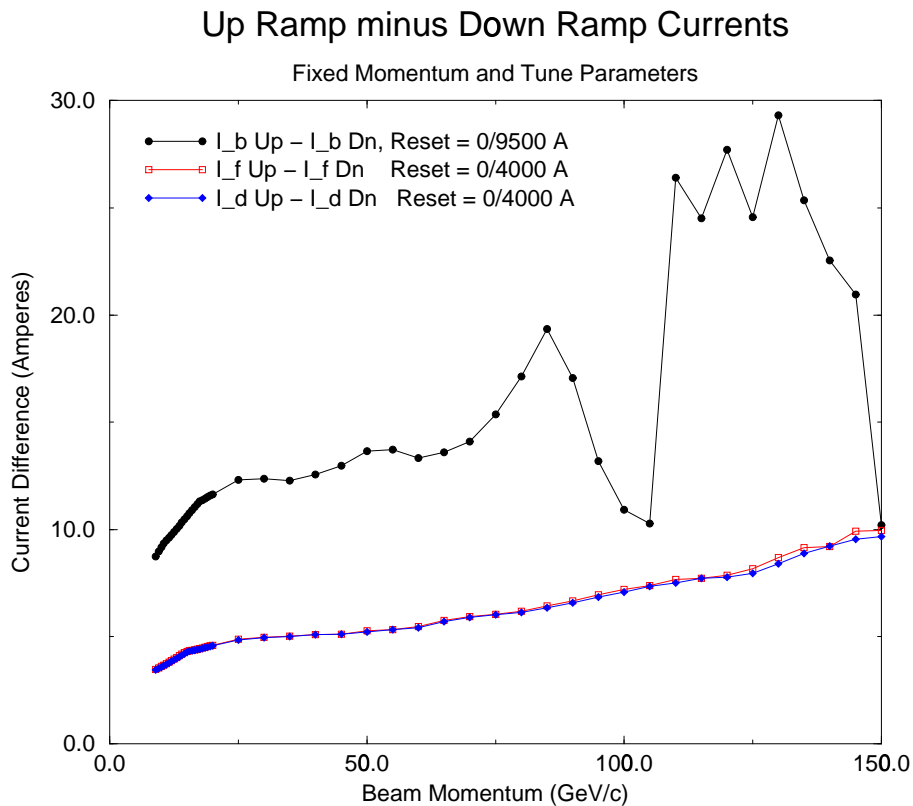


Figure 3: Difference (up - dn) in current required for the same momentum and tune on up ramp and down ramp. Note that the dipole downramp data is not adequate.

Another way to explore the effects which must be accounted for in controlling the dipole and quadrupole currents is to examine the differences in currents which produce the same fields. We do this at a variety of momenta,

requiring again that the design tune be achieved. We plot this results in Figure 3. Note that the data for dipole downramp which was selected in this study is of poor quality so the results plotted above about 60 A should be discounted. However below that point for dipoles and at all currents for quadrupoles, the difference grows slowly and monotonically with momentum (current). In planning the control strategies, we should be sure that this feature is not masked by assumptions which could add difficulty to the task of deceleration.

5 Hysteresis Fitting

To relate magnetic fields to the current required to produce them, the power supply control application will use an analytic model of the relation between magnetic field integral and current history. A preliminary fit to the hysteresis studies on BQB310-1 and IDA114-0 has been carried out and will be reported here. Improved fits are required.

5.1 General Properties

If one subtracts from the measured integrated strength, the field generated by the current in the existing geometry by ideal iron (this term is linear in I_{meas}), the non-linear term remaining is related to the H of the steel by geometric constants. The measurements we have made show two simplifications from the most general hysteretic properties which are reported on magnet steel. Since we only power the magnets to positive currents, we have major hysteresis loops which only go from near $H = 0$ to a maximum H . Our minor loops seem to asymptotically approach these curves even when we reverse current at arbitrary points between the extreme values of H .

- The first simplicity we observe is that the differences in asymptotic loops can be ignored and we can fit for curves (we designate them as Hysteresis Curves) with only one up ramp curve and one down ramp curve.
- The other simplifying factor is in the transitional curves which join up ramp and down ramp Hysteresis functions. We designate these as Interjacent Curves. We find that these curves have the same general shape for up to down transitions as for down to up transitions, they are all of a shape which is roughly exponential and to a useful degree,

all are characterized by the same parameters. Only when we have a satisfactory detailed fit will we know if the parameters are completely independent of the transition direction or of the current where the change in ramp direction is made.

Hysteresis studies have been done systematically with ramps which explore various reset currents for each ramp direction.

5.2 Measured Hysteresis Response and Fits

Nonlinear Integrated Dipole Strength

IDA114-0 (Fit with one Exp Interjacent) Downramp Study

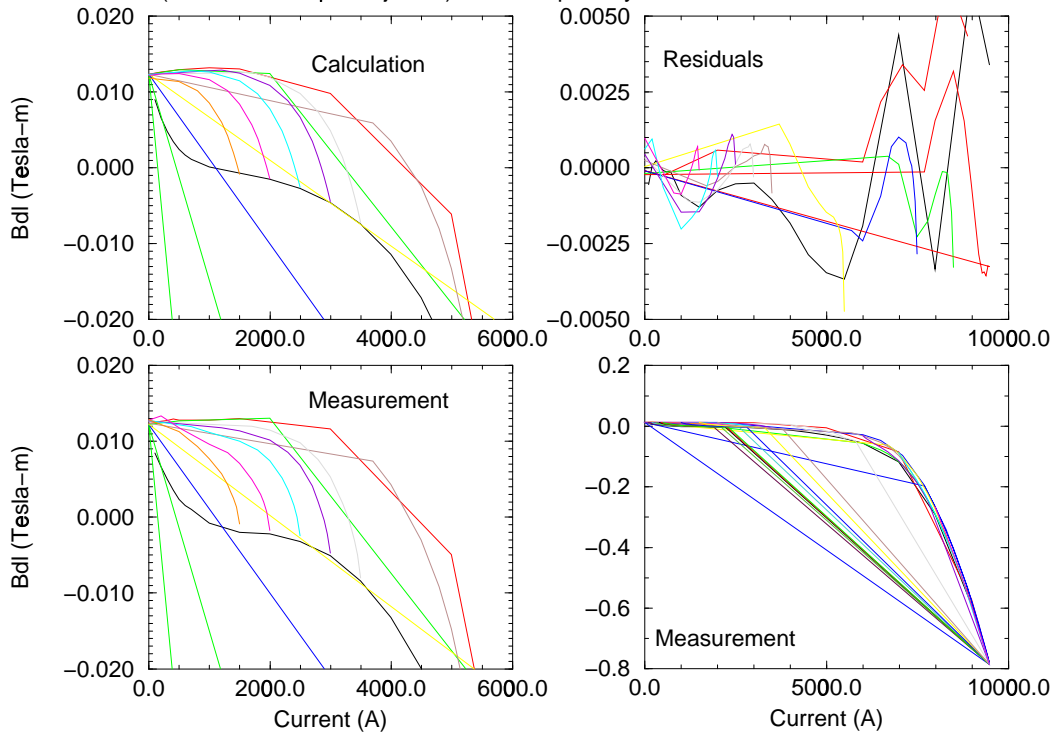


Figure 4: Measured and Fit non-linear integrated strength of IDA114-0 with various downramp reset currents.

Nonlinear Integrated Dipole Strength

IDA114-0 (Fit with one Exp Interjacent) Up-ramp Study

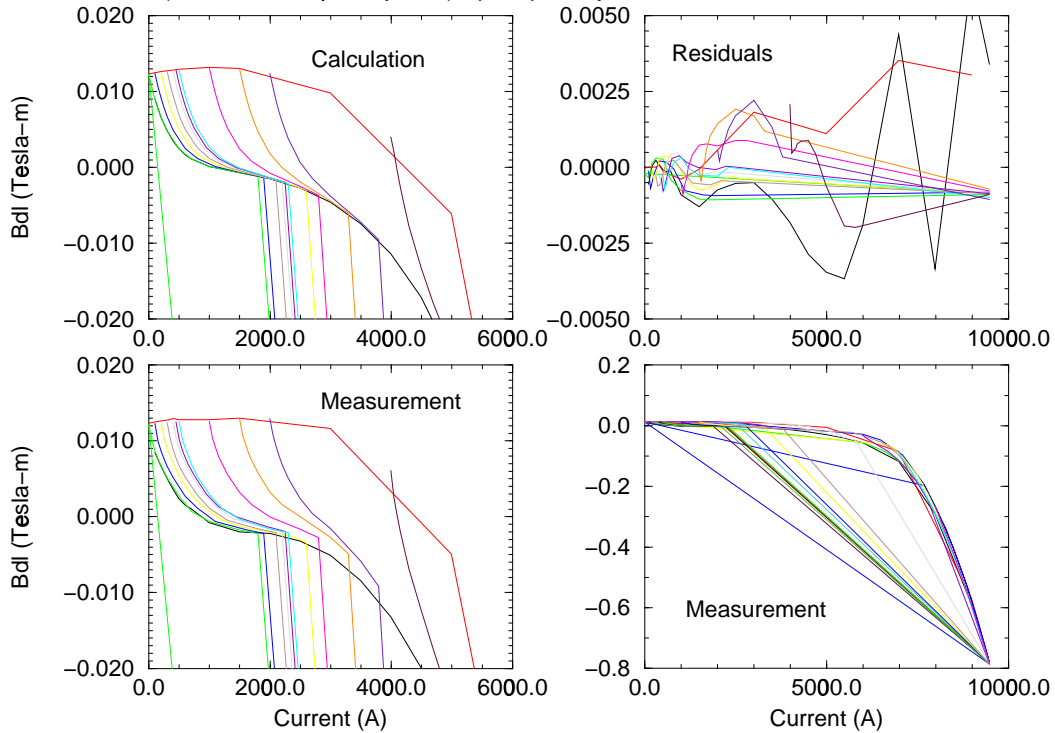


Figure 5: Measured and Fit non-linear integrated strength of IDA114-0 with various upramp reset currents.

A set of measurements of magnet strength were carried out for IDA114-0 and IQB310-1 which employed a set of currents with increasing (or decreasing) levels of reset current before upramp (downramp) measurements. The data were spaced following a fixed pattern of offset current from the reset current value. Measurements were carried out at MTF using the CHISOX[4] measurement system. Data from the harmonics.harmonics_red_runs table were extracted and organized into sets of ramps using a perl script. These magnets were also subjected to the standard set of measurements for Main Injector magnets of this series. The linear coefficient of a fit to Bdl vs. I was obtained from a fit to the lower current points of the standard down-

Nonlinear Quadrupole Strength

IQB310-1 (preliminary fit) Downramp Study

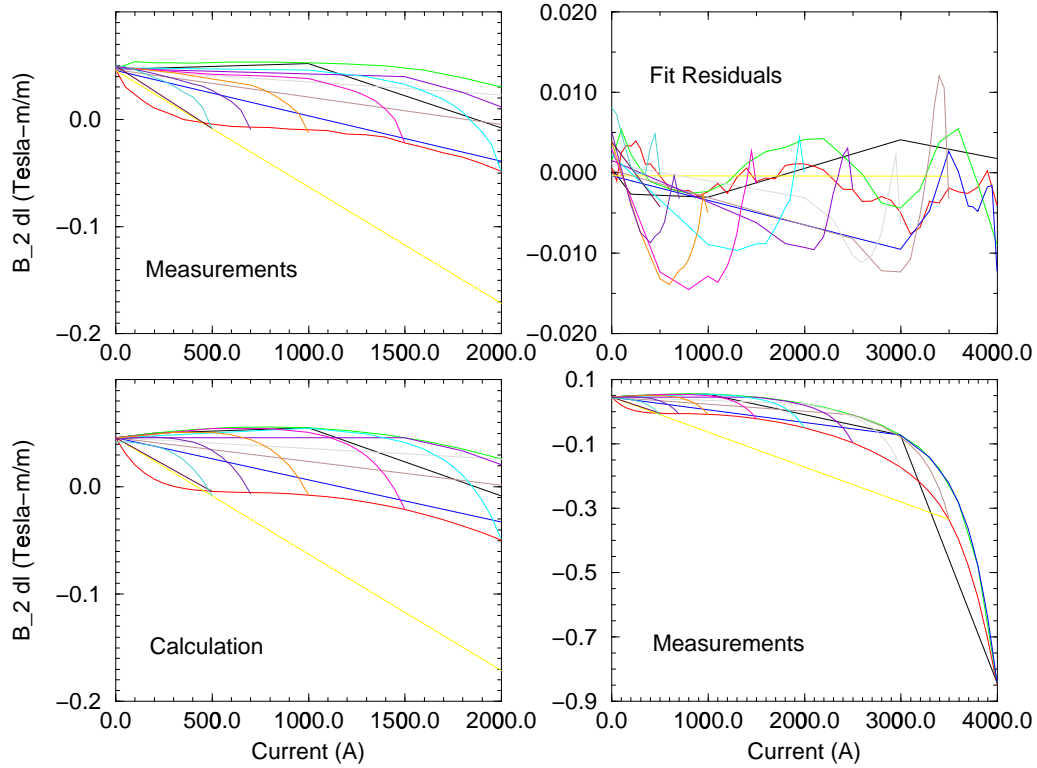


Figure 6: Measured and Fit non-linear integrated strength of IQB310-1 with various downramp reset currents.

ramp measurement. This term was then subtracted from the measured field integral using the measured current for I except where zero current was requested in which case the power supply is assumed to have produced zero current. The scale of the data is made suitable for presentation when the linear term is subtracted. Figures 4, 5, 6, and 7 show the measured non-linear fields in the lower left plot (upper left for quadrupoles) and on a less expanded scale on the lower right.

Parameterizations of the three curves are as follows:

- Linear (Electromagnet) Curve

$$Bdl_{lin}(I) = (Slope) * I \quad (13)$$

Nonlinear Quadrupole Strength

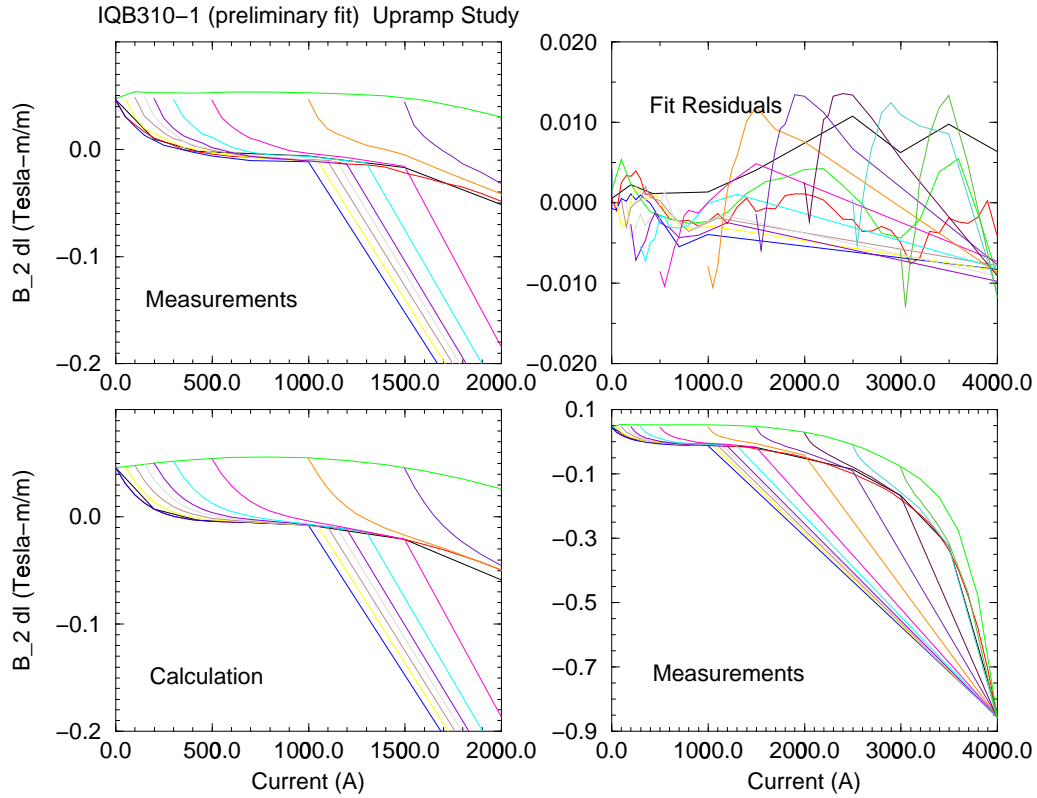


Figure 7: Measured and Fit non-linear integrated strength of IQB310-1 with various upramp reset currents.

- Hysteresis Curve

$$Bdl_{Hyst}(I, (dir)) = [C_0 + C_2 I_s] + [H_1 I_s - \sqrt{(H_1 - H_2)^2 I^2 + C}] \quad (14)$$

where $I_s = I/I_{scale}$, and the coefficients C_0, C_2, H_1, H_2 , and C have distinct values for upramp and down ramp hysteresis curves.

- Interjacent Curve

$$Bdl_{Inj}(I) = A_{Inj} e^{-(I - I_{reset})/ichar(dir)} \quad (15)$$

where I_{reset} is the most recent current at which the ramp direction was changed and for the up ramp, $A_{Inj} = Bdl_{Hyst}(I, up) - Bdl_{Hyst}(I, dn)$

is the difference in field between the downramp and upramp hysteresis curves evaluated at the reset current. For downramps, A_{Inj} has the opposite sign.

For IQB310, a subset of the data was fit using the NFIT program (a GUI interface to MINUIT). The full data set for IDA114 was fit with this parameterization using a FORTRAN program which called the MINUIT subroutine package. Using a perl script to manipulate the data and xmgr for creating plots, the fit parameters were used to plot the fitted results the residuals (measured minus fit) for both magnets at each of the measured currents.

The parameters obtained for these fits and used for the plotting program are shown in Tables 2 and 3.

Magnet IDA114-0				
Hysteresis HypPar1				
1	Slope	0.12041E-02	fixed	NaN
2	Iscale	10000.	fixed	NaN
3	Idn	7431.3	0.88319	0.12412E-01
4	Hdns1	-1.6843	0.10970E-02	-0.14469E-04
5	Hdns2	-0.35229E-01	0.63556E-03	-0.13378E-05
6	Cdn	0.28904E-01	0.12671E-03	0.79892E-06
7	Coeff0dn	0.22405E-01	0.24135E-03	0.27126E-06
8	Coeff2dn	-0.44337E-01	0.51163E-03	-0.20101E-05
9	ichardn	453.22	0.67519	-0.35841E-02
10	Iup	7885.5	0.56305	-0.64630E-02
11	Hups1	-2.2452	0.61632E-03	0.69469E-05
12	Hups2	0.47087E-01	0.81470E-03	-0.14389E-05
13	Cup	0.10944	0.28929E-03	-0.18210E-05
14	Coeff0up	0.66404E-01	0.33678E-03	-0.13116E-05
15	Coeff2up	-0.72650E-03	0.64762E-03	-0.20016E-06
16	icharup	350.08	0.74211	0.13127E-02

Table 2: Parameters for crude fit to IDA114-0 hysteresis studies.

Magnet IQB310-1				
Hysteresis HypPar1				
1	Slope	0.12254E-01	fixed	NaN
2	Iscale	10000.	fixed	NaN
3	Idn	3874.6	0.88319	0.12412E-01
4	Hdns1	-14.229	0.10970E-02	-0.14469E-04
5	Hdns2	-0.77145	0.63556E-03	-0.13378E-05
6	Cdn	0.28661	0.12671E-03	0.79892E-06
7	Coeff0dn	-0.12485E-01	0.24135E-03	0.27126E-06
8	Coeff2dn	-1.4203	0.51163E-03	-0.20101E-05
9	ichardn	180	0.67519	-0.35841E-02
10	Iup	3746.6	0.56305	-0.64630E-02
11	Hups1	-10.300	0.61632E-03	0.69469E-05
12	Hups2	-1.3797	0.81470E-03	-0.14389E-05
13	Cup	0.12005	0.28929E-03	-0.18210E-05
14	Coeff0up	-0.17799	0.33678E-03	-0.13116E-05
15	Coeff2up	-2.4447	0.64762E-03	-0.20016E-06
16	icharup	180	0.74211	0.13127E-02

Table 3: Parameters for crude fit to IQB310-1 hysteresis studies.

5.3 Discussion of Fit Results

In MI-0211[2], a specification was given for the fidelity with which the fitted results needed to match the magnet performance. This crude fit provides a very useful description of the data and permits one to see important effects, but falls short of the desired fidelity at both low and high fields by a factor of several. Nevertheless, we can draw a number of useful conclusions.

- This parameterization has the correct general properties at all field levels.
- Using a single exponential for the Interjacent Curve seems to leave a residual which has a characteristic shape in common for various reset currents for both up and down ramps. It appears that the fit would be improved with a second exponential term with larger characteristic current.

- It appears that at this level of examination, the use of the same parameters for all Interjacent Curves is satisfactory. Further examination will be required to determine if the differences between upramp and downramp are significant.
- The high field fits appear to be limited by the use of only hyperbola and parabola terms. Addition of one or more terms will likely permit a substantially better fit at high fields.

It is expected that efforts to modify the program so that more complex fitting can be attempted will begin soon.

6 Conclusions

Description of the magnetic field properties of Main Injector magnets in a way which permits the power supply control program to properly take into account the saturation and hysteresis of the magnets has achieved a substantial degree of success. The present characterization of the measured data fall short of the precision which would permit one to use it without any tuning parameters. However, the residual errors in this description have a pattern which suggests that the analytic approach will be adequate for machine control.

References

- [1] B.C. Brown, C. M. Bhat, D. J. Harding, P. S. Martin, and G. Wu. Design for Fermilab Main Injector Magnet Ramps Which Account for Hysteresis. In *Proceedings of the 1997 Particle Accelerator Conference (to be published)*, 1997. Also available as FERMILAB-Conf-97/147.
- [2] Bruce C. Brown. MI Power Supply Control Issues for Magnets with Hysteresis. Main Injector Note MI-0211 Ver 1.1, Fermilab, June 1997.
- [3] Dave Johnson. Main Injector Quad Length Ratios and Current *vs.* Tune Parameters. Main Injector Note MI-0185, Fermilab, July 1996.
- [4] J.W. Sim, R. Baiod, B.C. Brown, E. Desavouret, H.D. Glass, P.J. Hall, D.J. Harding, C.S. Mishra, J.M. Nogiec, J.E. Pachnik, A.D. Russell, K Trombley-Freytag, and D.G.C. Walbridge. Software for a Database-Controlled Measurement System at the Fermilab Magnet Test Facility.

In *Proceedings of the 1995 IEEE Particle Accelerator Conference, Dallas, May 1-5, 1995*, page 2285. Institute of Electrical and Electronic Engineers, 1995.